Dental Materials

The effect of high-intensity rapid polymerization on degree of conversion, monomer elution, polymerization shrinkage and porosity of bulk-fill resin composites

--Manuscript Draft--

Manuscript Number:	
Article Type:	Full Length Article
Keywords:	Bulk-fill; Rapid light-curing; Degree of conversion; Monomer elution
Corresponding Author:	Edina Lempel, DMD, PhD University of Pecs Medical School Faculty of Dentistry Pécs, HUNGARY
First Author:	Edina Lempel, DMD, Ph.D.
Order of Authors:	Edina Lempel, DMD, Ph.D.
	Donát Tamás Szebeni
	Zsuzsanna Őri, Ph.D.
	Tamás Kiss
	József Szalma, DMD, Ph.D., DSc
	Bálint Viktor Lovász, MD, DMD, Ph.D.
	Sándor Kunsági-Máté, Ph.D., DSc
	Katalin Böddi, Ph.D.
Abstract:	Objective The purpose was to compare the degree of conversion (DC), monomer elution (ME), polymerization shrinkage (PS) and porosity of two addition-fragmentation chain transfer (AFCT) modified resin-based composites (RBC) light-cured with rapid- (RP), turbo- (TP) or conventional polymerization (CP) settings. Methods Cylindrical samples (6-mm wide, 4-mm thick) were prepared from Tetric PowerFill (TPF) and Filtek One Bulk (FOB). Four groups were established according to the polymerization settings: 3s-RP, 5s-TP, 10s-CP and 20s-CP. Samples in 1mm thickness with 20s-CP settings served as controls. The DC at the top and bottom surfaces was measured with micro-Raman spectroscopy. ME was detected with high-performance liquid chromatography. PS and porosity were analyzed by micro-computed tomography. ANOVA and Tukey's post-hoc test, multivariate analysis and partial eta-squared statistics were used to analyze the data ($p<0.05$). Results FOB showed higher DC values (61.5%-77.5%) at the top compared to TPF (43.5%-67.8%). At the bottom TPF samples achieved higher DCs (39.9%-58.5%) than FOB (18.21%-66.18%). Extending the curing time increased DC (except the top of FOB) and decreased ME. BisGMA release was the highest from both RBCs. The amount was three-fold more from TPF. The factor Material and Exposure significantly influenced DC and ME. PS (1.8-2.5%) did not differ among the groups and RBCs except for the lowest value of TPF cured with the 3s_RP setting ($p=0.03$). FOB showed 4.5-fold lower porosity ($p<0.001$). Significantly higher pore volume was detected after polymerization in 3s_RP ($p<0.001$). Significance RP provided inferior DC values, increased ME and porosity of both investigated RBCs, and decreased PS in TPF.

Corresponding author: Edina Lempel, DMD, PhD, Habil.
Department of Restorative Dentistry and Periodontology,
University of Pécs Medical School
Tüzér street 1, Pécs, Hungary, H-7624

Editorial Board
Dental Materials

Dear Professor Watts,

I am writing to you regarding to our current manuscript submission entitled "**The effect of high-intensity rapid polymerization on degree of conversion, monomer elution, volumetric change and porosity of bulk-fill resin composites***"*.

Please consider our paper, which reports data about the degree of conversion, monomer elution, polymerization shrinkage and closed porosity of two addition-fragmentation chain transfer modified bulk-fill resin-based composite materials. Our paper would provide information about the effect of different curing modes, including rapid, turbo and conventional settings on the investigated parameters.

All of the authors have read the paper in its present form and approved its contents. The manuscript is submitted only for publication to the Dental Materials.

We hope this study should provide interesting and useful information for dentists in everyday dental practice.

Please let me know if you would require any changes to the manuscript to make it publishable in your excellent journal.

07.10.2022.

Yours Sincerely,

Edina Lempel DMD, PhD, Habil.

The effect of high-intensity rapid polymerization on degree of conversion, monomer elution, volumetric change and porosity of bulk-fill resin composites

Edina Lempel [a,*], Donát Szebeni [a], Zsuzsanna Őri [b,c], Tamás Kiss [b], József Szalma [d], Bálint Viktor Lovász [d], Sándor Kunsági-Máté [b,e], Katalin Böddi [f]

a) Department of Restorative Dentistry and Periodontology, University of Pécs Medical School, Pécs, Tüzér street 1, 7623-Hungary

b) János Szentágothai Research Center, Pécs, Ifjúsag Street 12, 7624-Hungary

c) Department of General and Physical Chemistry, University of Pécs, Pécs, Ifjúság Street 6, 7624-Hungary

d) Department of Oral and Maxillofacial Surgery, University of Pécs Medical School, Pécs, Tüzér street 1, 7623-Hungary

e) Department of Organic and Medicinal Chemistry, University of Pécs, Faculty of Pharmacy, Pécs, Honvéd Street 1, 7624-Hungary

f) Department of Biochemistry and Medical Chemistry, University of Pécs Medical School, Pécs, Szigeti Street 12, 7624-Hungary

*** Corresponding Author:**

Edina Lempel D.M.D., PhD, Habil., Associate Professor

Department of Restorative Dentistry and Periodontology, University of Pécs Medical School

Tüzér Street 1, Pécs, Hungary, H-7623

Tel: +36 72 502434

e-mail: lempel.edina@pte.hu

The effect of high-intensity rapid polymerization on degree of conversion, monomer elution, polymerization shrinkage and porosity of bulk-fill resin composites

Objective. The purpose was to compare the degree of conversion (DC), monomer elution (ME), polymerization shrinkage (PS) and porosity of two addition-fragmentation chain transfer (AFCT) modified resin-based composites (RBC) light-cured with rapid- (RP), turbo- (TP) or conventional polymerization (CP) settings.

Methods. Cylindrical samples (6-mm wide, 4-mm thick) were prepared from Tetric PowerFill (TPF) and Filtek One Bulk (FOB). Four groups were established according to the polymerization settings: 3s-RP, 5s-TP, 10s-CP and 20s-CP. Samples in 1mm thickness with 20s-CP settings served as controls. The DC at the top and bottom surfaces was measured with micro-Raman spectroscopy. ME was detected with high-performance liquid chromatography. PS and porosity were analyzed by micro-computed tomography. ANOVA and Tukey's post-hoc test, multivariate analysis and partial eta-squared statistics were used to analyze the data ($p<0.05$).

Results. FOB showed higher DC values (61.5%-77.5%) at the top compared to TPF (43.5%-67.8%). At the bottom TPF samples achieved higher DCs (39.9%-58.5%) than FOB (18.21%-66.18%). Extending the curing time increased DC (except the top of FOB) and decreased ME. BisGMA release was the highest from both RBCs. The amount was three-fold more from TPF. The factor *Material* and *Exposure* significantly influenced DC and ME. PS (1.8-2.5%) did not differ among the groups and RBCs except for the lowest value of TPF cured with the 3s_RP setting ($p=0.03$). FOB showed 4.5-fold lower porosity ($p<0.001$). Significantly higher pore volume was detected after polymerization in 3s_RP ($p<0.001$).

Significance. RP provided inferior DC values, increased ME and porosity of both investigated RBCs, and decreased PS in TPF.

Keywords: Bulk-fill, Rapid light-curing, Degree of conversion, Monomer elution

1. Introduction

The polymerization of resin-based composite (RBC) restorative materials is induced by light curing units (LCU) at distinct power densities and exposure times. The product of power density (irradiance level) and exposure duration gives the radiant exposure or total radiant energy [1]. For RBCs, a minimum radiant exposure is required for adequate polymerization, however, above a certain level, which is specific for the material, the degree of conversion cannot be increased [1-3]. The exposure reciprocity law states that for a given radiant exposure, the degree of conversion (DC) from monomers to polymers (i.e. polymerization) does not change with any combination of irradiance and exposure time [4]. Based on this concept, the request from the clinicians for shorter exposure time encouraged the manufacturers to increase the radiant emittance of LCUs [5]. However, the validity of the reciprocity law has proved controversial and has been dismissed, as it depends on the photoinitiator- and monomer-system present in the RBC, the spectral radiant power of the LCU and exposure time [6-10]. Reactions, such as radical polymerization will not follow the reciprocity law, which requires first order dependence, as they are inherently non-linear in their dependence on light intensity [10]. Wydra et al. found in an experimental resin composite model, that the monomer-to-polymer conversion decreased at a constant irradiation dose as irradiation intensity increased, and the overall dose required to achieve full conversion also increased. Furthermore, besides the ultimate conversion, shrinkage stress levels were dependent not only upon dose but also the irradiation intensity, in contrast to an idealized reciprocity relationship [10]. The above referred findings show that different irradiation conditions with the same overall dose can result in significantly different DCs and shrinkage stress. However, Palagummi et al. has established empirically, that if the radiant exposure is above the minimum, the exposure reciprocity law is valid with respect to the DC of RBCs with a filler content of more than 50 weight % [2]. This demonstrates, that the validity of the reciprocity law is dependent not only upon how the polymerization rate scales with the light intensity but also the composition of the polymerizing material. To provide the desired reduction in the curing time, modifications in the RBC composition are necessary. Conventional photopolymerization of cross-linking monomers can be described as a radical chain growth polymerization, leading to materials with less controlled and heterogeneous network architecture [9, 11]. In the rapid initiation reaction, a large number of photoinitiators are activated producing a large number of free radicals. The high concentration of free radicals annihilate each other, thus reducing the possibility of further activation of monomer

species and propagation of radical polymerization. Uncontrolled free-radical polymerization results in relatively broad chain-length distribution and ill-defined end-groups with decreased DC and unreacted monomers trapped within the polymer network [12]. Many of these issues might be resolved through the use of a chain polymerization from which termination is absent. This so-called living polymerization is feasible with the incorporation of a reversible addition-fragmentation chain transfer (RAFT) molecule where an active center effectively diffuses throughout the network, simultaneously creating free radicals that initiate a new propagating radical and enables bond rearrangement [12-14]. The exchange reaction between a trace amount of growing radicals and a transfer agent that acts as the dormant species proceeds by an appropriate RAFT agent, typically a thiocarbonylthio compound [12]. The benefits of the RAFT polymerization include more homogenous polymer network, increased DC, decreased shrinkage and shrinkage stress, increased toughness, and the ability of acting as covalent adaptable networks (e.g., shape memory polymers) [12].

The RAFT-modified chemistry of RBCs was apparently sufficient to enable very short light exposure time (3 s) with high radiant exitance (> 3000 mW/cm^2) without adverse consequences, as reported in some studies that investigated these newly introduced restorative materials (i.e. Tetric PowerFill, Ivoclar Vivadent AG, Schaan, Liechtenstein) [15-19]. These studies found, that the Vickers hardness, DC, depth of cure, flexural strength, and modulus did not differ significantly from the RBC with the same composition but without the β-allyl sulfone as RAFT reagent.

The application of addition-fragmentation chain transfer (AFCT) molecule in RBCs is not unique to Tetric PowerFill, as a similar approach is employed in Filtek One Bulk Restorative (3M ESPE, St. Paul, MN, USA). In this RBC the addition-fragmentation is achieved through a complementary internal double bond with a β-quaternary carbon center functional group (free radical species) embedded within the proprietary terminal methacrylate monomer necessary for crosslink formation [20]. The incorporation of this addition-fragmentation monomer (AFM) aimed to relax stress during polymerization via network reconfiguration [20]. Shah et al. found in an experimental RBC, that the AFM utilized in the dimethacrylate networks serves as a useful and potent additive to reduce shrinkage stress in polymerizing networks [20]. However, the AFM can impair the DC in a concentration-dependent manner due to production of radical species with increased stability in methacrylate networks. This reduction in DC at low level of AFM (< 5%) and under higher

irradiance conditions is minor while the corresponding reduction in stress is significant [20]. Par et al. compared the shrinkage stress of Tetric PowerFill to Filtek One Bulk Restorative, and to other contemporary and bulk-fill RBCs and found, that the two materials employing the AFCT chemistry demonstrated the lowest shrinkage forces [17]. However, it was also concluded, that the ultra-fast photopolymerization can lead to considerably faster development of shrinkage forces in the early stage of polymerization. Furthermore, the higher versatility of crosslinking density in rapid high-radiant exitance curing resulted in inferior mechanical properties at the bottom of the specimens and decreased resistance to aging [17, 21]. The gradual decrease in crosslinking density in deeper regions is most likely related to light attenuation. Light attenuation is dependent on the reflection on filler particles; absorption by photoinitiators, and pigments; changes in refractive indices, and temperature during polymerization; as well as incorporated air bubbles in the RBC [22]. As light is attenuated within the material, the monomer-to-polymer conversion could be compromised and may lead to incomplete polymerization. Incomplete conversion results in unreacted monomer release, which may raise biocompatibility issues [23, 24]. The amount of unreacted monomers could be higher in the presence of porosities containing oxygen and may potentially be released as a result of solubilization, and increased water sorption [25].

As it was stated by Moad et al., living polymerization has further limitations such as the limited compatibility with very few monomers, reduced photoreactivity, intolerance of many types of functionality, sensitivity to trace amounts of impurities, and requires strictly controlled polymerization circumstances [12]. According to the above limitations, the polymerization of AFCT containing RBC's is very difficult and strongly depend on the composition of the RBC, and polymerization conditions.

The aim of the present study was to determine the effect of different curing protocols on DC, monomer elution, volumetric shrinkage, and internal porosity of AFCT modified bulk-fill RBCs, including an RBC specifically designed for high-intensity light-curing. The first null-hypothesis assumed no effect of curing protocol on the following properties: (1) DC, (2) monomer elution, (3) volumetric shrinkage, and (4) internal porosity. The second hypothesis assumed that there are no significant differences between the materials regarding the aforementioned properties.

2. Materials and Methods

2.1.Resin composites and radiant exposures

During this in vitro study two brands of AFCT molecule containing bulk-fill RBCs were analyzed. The brand, the chemical composition and the manufacturer are presented in Table 1. According to the sample preparation and polymerization method, specimens were divided into five experimental groups. In each group, from each material, 5 further specimens were prepared. Table 2. shows the experimental groups according to the method of polymerization, the abbreviations of the investigated materials, and the delivered radiant energy.

The samples were prepared in a cylindrical polytetrafluoroethylene (PTFE) mold with an internal diameter of 6 mm, external diameter of 12 mm, and a height of 4 mm, meanwhile, the control group thickness was 1 mm, provided by 1 mm height of the mold. A polyester strip was positioned between the mold and the glass slab under the molds. A capsule dispenser gun was used to apply the bulk-fill RBCs into the mold. Before irradiation, the RBC sample was covered with a polyester strip to avoid contact with oxygen. All specimens were irradiated with Light Emitting Diode (LED) curing unit (Bluephase PowerCure, Ivoclar Vivadent, Schaan, Liechtenstein; ʎ = 385-515 nm; 10 > 9 mm exit diameter fiberglass light guide) in different polymerization settings (Table 2), powered by a line cord at room temperature. The tip of the fiberglass light guide was in direct contact, centrally positioned and parallel to the mold. A silicone key was made to ensure the reproducible positioning of the light guide. The irradiance of the LED unit was monitored before and after polymerization with a radiometer (Bluephase Meter, Ivoclar Vivadent, Schaan, Liechtenstein) by placing the tip directly at a distance of 0 mm from the radiometer sensor. The radiant exposure (J/cm^2) was calculated with the product of the irradiance (mW/cm^2) and the applied exposure time (s). To represent the irradiance delivered to the top of the RBCs the light attenuation of the 6 mm orifice of the mold was also measured by interpositioning a black paper with a 6 mm diameter hole between the mold and the sensor. The tip of the LCU was placed directly over the hole above the sensor.

2.2. Micro-Raman spectroscopy measurements

The prepared samples were stored in dark in an incubator (Cultura, Ivoclar Vivadent, Schaan, Liechtenstein) at 37 ± 1 °C and 90% ± 10% relative humidity. 24 h post-cure DC values were evaluated with a confocal Raman spectrometer (Labram HR 800, HORIBA Jobin Yvon S.A.S., Longjumeau Cedex, France). The parameters of the measurements were set according to the following: 20 mW He-Ne laser with 632.817 nm wavelength, magnification x 100 (Olympus UK Ltd., London, UK), spatial resolution ~15 µm. The two peaks analyzed at 1639 cm^{-1} and 1609 cm^{-1} were ~30 cm^{-1} apart, thus the spectral resolution of ~2.5 cm^{-1} provided satisfactory results. Spectra were taken at the center, at the periphery, and between these two regions of each RBC sample both from the top and bottom surfaces with an integration time of 10 s. Ten recordings were averaged for each geometrical point. Spectra were taken from non-polymerized RBC as reference. LabSpec 5.0 (HORIBA Jobin Yvon S.A.S., Longjumeau Cedex, France) dedicated software was used for the analysis and post-processing of the spectra. The DC was calculated by comparing the relative change of the integrated band intensities at 1639 cm^{-1} (aliphatic C=C bonds) and the reference band at 1609 cm^{-1} (aromatic C=C bonds) of non-polymerized and polymerized RBC samples. DC was calculated by including the values of the integrated intensities in the following formula:

$$DC\% = (1 - (R_{cured} / R_{uncured}))x100$$

where R is the ratio of peak intensities at 1639 cm^{-1} and 1609 cm^{-1} associated to the unconjugated and conjugated carbon bonds in non-polymerized and polymerized RBCs, respectively.

2.3. Reversed-phase high performance liquid chromatography measurements

After the irradiation, the samples were immersed into 1.0 mL of 75% ethanol/water storage medium in separate glass vials and stored in a 37 °C incubator. According to the ISO 10993-13 description, the ratio between the sample and the storage solution volume was greater than 1:10, hence, the specimens were kept fully immersed in the medium for 72h. Solutions were then collected for the qualitative and quantitative analysis of the eluted unreacted monomers. Reversed-phase high performance liquid chromatography (RP-HPLC) was used for the analysis. The RP-HPLC system (Dionex Ultimate 3000, Thermo Fisher Scientific Inc, Sunnyvale, CA, USA) consists of a Dionex LPG 3400 SD gradient pump, Rheodyne injector (Rheodyne, California, USA) and a Dionex DAD 3000 RS UV–VIS detector (Dionex GmbH, Germering, Germany). Data was

collected using the Chromeleon software (version: 7.2.10). The separations were performed on a Brisa "LC^{2}" (particle size: 5 μm) (Teknokroma, Sant Cugat del Vallés, Spain) column (250 mm x 4.60 mm) with gradient elution. The composition of Eluent "A" was 100% bidistilled water, whereas Mobile Phase "B" was 100% v/v acetonitrile (ACN) (VWR International, USA). During the 30-min chromatographic separation, the "B" eluent content was increased from 40% to 95%. The flow rate was 1.2 mL x min^{-1}. For the regeneration of the stationary phase, the content of Mobile Phase B was decreased from 95% to 40% in 1 min, and after 31-46 min, the system was washed with 40% "A". The detection of the eluted monomers was carried out at the following wavelengths: 205, 215, 227 and 254 nm. 205 nm was found to be optimal; therefore, the evaluation relied on the data collected at this wavelength. The separations were undertaken at room temperature. The amounts of the eluted monomers (bisphenol A-glycidyl methacrylate, BisGMA; trietylene-glycol-dimethacrylate, TEGDMA; urethane-dimethacrylate, UDMA; 1,12-dodecanediol-dimethacrylate, DDDMA and tricyclodecane-dimethanol-dimethacrylate, TCDDMA) were calculated using the calibration curve with the areas under the curve of peaks produced by the monomers, respectively. Monomer release was calculated to 1 mg RBC. TEGDMA, UDMA, BisGMA, TCDDMA, DDDMA standard solutions had retention times of 11.07, 16.10, 18.42, 23.39, and 29.20 min, respectively, while the peaks were well separated from each other.

2.4. Micro-computed tomography measurements

The cylindrical mold (6 x 1 mm and 6 x 4 mm) filled with the uncured RBC was covered with a black topper to inhibit the pre-polymerization of the samples and micro-computed tomography (micro-CT) scans were performed (Skyscan 1176, Bruker, Kontich, Belgium). Each sample was scanned for approximately 36 minutes. After the first scan, each sample was removed from the scanner using a sample holder and polymerized using the Bluephase PowerCure LED curing unit. During the second scan a reference mark over the micro-CT platform ensured the same position of the samples. Five samples were scanned from each group before and after polymerization and volumetric shrinkage was calculated. Overall, 100 micro-CT readings were acquired from 50 scanned samples. The operating energy (80 kV, 350 μA), resolution (8.74 μm/slice), rotation step (0.7°), exposure time (1500 ms), and the filter (Al 1mm) for the micro-CT device were kept

constant for all samples. The acquired raw images were reconstructed with the software (SkyScan reconstruction program, NRecon, v.1.7.4.2, Bruker) to correct for radiologic artefacts and prepare for analysis. Images were converted to 1404 × 1404 pixel resolution in *.bmp format. The 3D volumetric analyses of the reconstructed images were performed using the specific functions in the software (Skyscan software CTAn, v. 1.20.8.0, Bruker) according to the following workflow: raw image acquisition, identification of region of interest, binary selection, morphometry, and custom processing. The reconstructed images were also further processed for visualization (The Dataviewer, Skyscan). The region of interest (ROI) was determined after reconstruction by using the CT analyzer software for the 3D microarchitecture analysis of each specimen. ROI included the entire RBC sample within the mold.

Volumetric loss due to polymerization shrinkage was calculated as a percentage using the data of the post- and the pre-cured samples' volume.

The pores in 3D volumes were calculated using the grayscale images processed with a Gaussian low-pass filter for noise reduction. RBC samples were subtracted from the plastic mold image using an automatic segmentation threshold of the CT analyzer software. A global thresholding was used to process the gray level ranges to get an imposed image of only black and white pixels. The volume of internal void relative to total RBC specimen volume was calculated (%) by measuring the internal voids and specimen volumes of each RBC sample.

2.5. Statistical analysis

The statistical analyses were performed with SPSS (Version 26.0; IBM, Armonk, NY, USA). Kolmogorov-Smirnov test was applied to test the normal distribution of the data, followed by a parametric statistical test. The differences in DC between the top and bottom were analyzed by paired sample t-test. The monomer elution, volumetric change and porosity of the investigated RBCs were compared with one-way analysis of variance (ANOVA). Tukey's post hoc adjustment was used for multiple comparison in all ANOVA models. A two-tailed independent t-test was used to compare the difference between the similar subgroups of the two RBCs. Multivariate analysis (general linear model) and partial eta-squared statistics were used to test the influence and describe the relative effect size for *material* and *exposure* as independent factors. P values below 0.05 were considered statistically significant.

3. Results

3.1. Radiant exposure

The maximum and the attenuated radiant exitances of the LED LCU, and the delivered incident radiant exposures of the different curing modes are presented in Table 2. The radiant exposure was reduced by ~ 20% through the 6 mm orifice of the mold. The delivered radiant exposure to the top of the samples was similar in cases of the 3 s and turbo mode, higher by 1.6 J/cm^2 in case of the high mode for 10 s, meanwhile it was doubled with an exposure duration of 20 s (Table 2).

3.2.Micro-Raman spectroscopy measurements

Regarding the DC at the top and bottom surfaces of the samples, percentages ranged between 43.5 – 77.45% and 18.2 – 66.2%, respectively (Fig.1 and 2). Significantly higher DC values on the top surfaces were detected in favor of FOB, however, the opposite was found regarding the bottom surfaces, except in the control group (FOB_1_20). For both materials significant differences were found between the top and bottom DC values (Table 3). The DC values measured at both the top and bottom surfaces of TPF gradually increased as the exposure time was increased and the highest value was achieved in the control group (Table 4). While the bottom surface of FOB followed a similar scenario as TPF, the top surfaces did not show a proportional relationship with exposure duration (Table 5). The highest DC was detected in the control groups of both RBCs. The bottom to top DC ratio (R-DC) of FOB was much lower (24.4 – 63.5%) compared to TPF (79.6 – 91.7%), except in the case of the control groups. The highest R-DC was achieved in the 3 s group for TPF (91.7%), however, the top and bottom DC values of TPF were the lowest in this group. As the exposure duration increased the R-DC decreased, except for TPF_1_20. On the contrary, for FOB, R-DC values showed a directly proportional increase with increasing exposure duration.

A *Material* x *Exposure* mixed-model ANOVA revealed that the main effect for *Material* was significant [F (1, 40) = 202.37, $p < 0.001$] and the Partial Eta-squared [(ηp^2) = 0.84] was considered to be large also. Similarly, the effect for *Exposure* was also significant [F (4, 40) = 39.34, $p < 0.001$], with large effect size ($\eta p^2 = 0.79$) on the DC values of the top surfaces. The interaction

(*Material x Exposure*) [F (4, 40) = 42.82, $p < 0.001$, $\eta p^2 = 0.81$] had large effect on the monomer conversion at the top.

Regarding the DC values at the bottom surfaces, the results showed significant and large effects both for factors *Material* [F (1, 40) = 124.04, $p < 0.001$, $\eta p^2 = 0.76$] and *Exposure* [F (4, 40) = 125.58, $p< 0.001$, $\eta p^2 = 0.926$]. The interaction (*Material x Exposure*) [F (4, 40) = 34.01, $p< 0.001$, $\eta p^2 = 0.77$] also significantly affected the monomer conversion at the bottom surfaces.

3.2. Reversed-phase High Performance Liquid Chromatography measurements

UDMA, BisGMA and TCDMA standard monomers were used for TPF and UDMA and DDDMA were selected to detect the elution of these monomers from FOB. In addition to the monomers specified by the manufacturers, other methacrylates were also detected from both TPF (TEGDMA) and FOB (BisGMA) RBCs. Although, TCDMA is a component of TPF, free monomer was not released in a detectable amount. The increasing exposure time significantly decreased the free monomer elution from both investigated RBCs (Fig.3). Regarding the monomer elution from the different groups in case of TPF, the following order can be set: TPF_20 < TPF_1_20 < TPF_10 < TPF_5 < TPF_3. The order of the eluted monomers from the different groups of FOB is similar to TPF (FOB_1_20 < FOB_20 < FOB_10 < FOB_5 < FOB_3), except the control group which released significantly lower amount of monomers compared to the group FOB_20. Among the released monomers, BisGMA was detected at the highest level from both investigated materials. The eluted amount was threefold more from TPF. The amount of UDMA release was similar for both RBCs. Although, TEGDMA is not described by the manufacturer's as a component, the elution of this dimethacrylate exceeded the UDMA release from TPF.

Mixed-model ANOVA showed that the main effect for *Material* was significant on UDMA and BisGMA release [F_{UDMA} (1, 40) = 1106.93; F_{BisGMA} (1, 40) = 59346.5; $p < 0.001$] and the Partial Eta-squared was considered to be large ($\eta p^2_{UDMA} = 0.97$; $\eta p^2_{BisGMA} = 0.99$). The *Exposure* factor influenced also significantly the monomer elution [F_{UDMA} (4, 40) = 5769.29, $p < 0.001$; F_{BisGMA} (4, 40) = 9084.33, $p < 0.001$] and the Partial Eta-squared was also considered to be large ($\eta p^2_{UDMA} = 0.99$; $\eta p^2_{BisGMA} = 0.99$). The interaction (*Material x Exposure*) had significant effect with large effect size both on UDMA [F_{UDMA} (4, 40) = 239.22, $p < 0.001$, $\eta p^2_{UDMA} = 0.96$] and BisGMA

[F_{BisGMA} (4, 40) = 1997.64, p < 0.001, ηp^2_{BisGMA} = 0.99] elution. Since TEGDMA was released only from TPF, while DDDMA was eluted from FOB, only the *Exposure* factor was analyzed. While significant [F_{TEGDMA} (1, 23) = 18.63, p < 0.001] effect was detected for this monomer elution with medium effect size (ηp^2_{TEGDMA} = 0.448), DDDMA [F_{DDDMA} (1, 23) = 1.96, p = 0.175, ηp^2_{DDDMA} = 0.078] elution was independent from the *Exposure* factor.

3.4. Micro-computed tomography measurement

For both materials tested, the sample volume after polymerization was significantly decreased compared to the uncured stage (p < 0.01), thus polymerization shrinkage occurred. However, the p-value corresponding to the F-statistic of one-way ANOVA for TPF and FOB is 0.7 and 0.25, respectively, suggesting that there is no significant difference in shrinkage among the subgroups. Comparing the RBCs, TPF showed statistically significant lower polymerization shrinkage in group TPF_3 according to the independent two tailed t-test [t(4) = 2.3; p = 0.03]. Volumetric shrinkage values are presented in Fig 4. The effect of both *Material* (p = 0.09) and *Exposure* (p = 0.18) was considered to be insignificant according to the results of the general linear model. The partial eta squared indicated a medium effect size of *Material* (ηp^2 = 0.08).

The average closed porosity values for pre-cured FOB were 3.5-fold lower (0.002%) compared to the values of TPF (0.007%) [t(4) = -5; p = 0.001], while the post-cure porosity values were 4.5-fold lower (FOB, 0.003%; TPF, 0.013%) [t(4) = -5.8; p < 0.001]. The closed porosity values did not differ significantly between the investigated pre- and post-cured groups within the same material (FOB, p = 0.09 or TPF, p = 0.06). However, significant difference was detected between the pre-cured and post-cured pore volume in groups with 3 s setting regarding both RBCs [FOB: t(4) = 5,2; p < 0.001; TPF: t(4) = -12.6; p < 0.001] (Fig.5). The multivariate general linear model revealed that the *Material* factor has a significant effect (p = 0.001) on closed porosity and the effect size was considered to be large (ηp^2 = 0.16). *Exposure* factor however, insignificantly (p = 0.12) affected the porosity with medium effect size (ηp^2 = 0.07).

4. Discussion

The AFCT methodology is a living/controlled free radical polymerization process. It is intended to control the relatively broad molecular mass distribution and end group functionality of the RBCs [12]. Addition-fragmentation was introduced recently in dentistry and applied in two bulk-fill RBCs so far. AFCT is attained through a complementary internal double bond with a β-quaternary carbon center functional group or by adding a β –allyl sulfone group as an RAFT agent [14, 20]. RAFT polymerization was reported to increase the DC and toughness, and decrease the shrinkage and shrinkage stress [12, 17]. The present *in vitro* study investigated the corresponding effects of different curing protocols on DC, monomer elution, volumetric shrinkage, and internal porosity of the two available AFCT molecule modified bulk-fill RBCs. Since all evaluated properties were affected by the curing protocol for the investigated RBCs, the first null hypothesis was rejected. The second null hypothesis was also rejected because the evaluated properties differed between the two AFCT modified RBCs.

The application of the addition-fragmentation methodology does not propose the usage of special monomer- and initiator system compared to a conventional free radical polymerization [12]. TPF composition is based, to a great extent, on the commercial RBC from the same company (TetricEvoCeram Bulk-Fill, Ivoclar Vivadent AG, Schaan, Liechtenstein) [15]. The organic matrix system of both materials is based on the monomers of UDMA, Bis-EMA and Bis-GMA, meanwhile TPF contains additionally a TCDDMA, a propoxylated bisphenol A dimethacrylate component and the AFCT molecule. Since the initiation and propagation of the polymerization process are similar in both RAFT and conventional radical polymerization, the polymerization of TPF is initiated in the same way using three different types of photoinitiators – camphoroquinone (CQ)/amine, an acyl phosphine oxide (TPO) and Ivocerin [bis-(4-methoxybenzoyl)diethylgermane] [15]. Ilie and Watts concluded, that the RAFT-modified material allowed a cure-time of 3 s at high irradiance and induced comparable properties to the RBC with a very similar composition with faster initial polymerization kinetics [15]. The slightly faster kinetic in the upper layers had no effect on the post-polymerization in view of the C=C double bond conversion. The DC measured 300 s post irradiation in the above study was similar in both materials with a value of ~ 45% irrespective of the curing mode [15]. The DC values of TPF in our study are comparable to the above corresponding findings. The DC at

the top and bottom surfaces of TPF increased proportionally with the increased exposure duration and radiant energy, however the results did not demonstrate a significant difference among all investigated groups. The lowest DC values were measured in groups of TPF_3 (39.9%) and TPF_5 (44.5%) with a calculated radiant exposure of 7.5 J/cm^2 and 7.8 J/cm^2, respectively. Significantly higher values were detected in the TPF_10 (48.5%) and TPF_20 (50.8%) groups. Par et al., who investigated the rapid (3 s, 10.3 J/cm^2) and conventional (10 s, 13.4 J/cm^2) curing modes, found DC values not to differ significantly with values of 45% and 50%, respectively [17]. Despite the fact that the investigated layer thickness was smaller and the transmitted energy was higher in relation to our investigation, almost the same DC values were obtained. In the TPF_20 group, the exposure duration and thus the radiant exposure was doubled (19 J/cm^2), however the corresponding DC difference was insufficient to produce a statistically significant result compared to the TPF_10 (9.4 J/cm^2) group. Marovic et al. found that TPF is evidently better cured at moderate radiant exitance with a longer exposure time. They explained it by the high molecular-weight AUDMA content, which most likely limits the mobility of the monomers in a rapidly forming network [26].

Although, it is well-documented, that a higher level of degree of cure could be achieved by increasing the energy density – mainly by extending the exposure time –, the present results did not confirm this statement regarding the DC values detected between groups of TPF_10 and TPF_20 [3, 27-29]. The polymerization kinetics have been found to be highly complex, and irradiance, exposure duration and composition can independently affect the DC [30, 31]. As an explanation, the initiator depletion may arise after an exposure duration of 10 s at deeper regions of 4 mm samples. The initiator system of TPF is based on CQ/amine, TPO and Ivocerin. The two latter have higher molar extinction coefficients, which result in faster initial curing kinetics and a greater consumption of initiator molecules [15, 32]. Our findings confirm previously reported results wherein plotting radical concentration against radiant exposure revealed a plateau following a short (3–5 s) exposure duration in TPO-containing RBCs [33]. It was concluded, that RBCs with TPO initiator did not benefit from an increase in irradiance and/or exposure time above a given threshold. These investigations determined the threshold to be at 3–6 J/cm^2 radiant exposure [34], however our findings showed the plateau at around 9 J/cm^2 at the bottom of the samples. The result of the bottom to top DC ratio calculation supports the above speculation since the value was found to be similarly the lowest in case of TPF_10

and TPF_20. The control specimens of 1 mm thickness irradiated with the same energy density (19 J/cm^2) provided the highest DCs, however this was not significant compared to the DC value of TPF_20. The control group was expected to be able to achieve the maximum value characteristic to TPF. In general, the top to bottom DC ratio was high in all TPF groups (R-DC: 78.6-91.7%) due to optimal wavelength ranges provided by the polywave curing unit encompassing the range of absorbance of the complex photoinitiator system in order to gain high degree of polymerization [35, 36]. In contrast, Hayashi et al. found the R-DC% to be below 80% in the case of TPF [19]. The present study measured the DC only at the top and bottom surfaces, and detected significantly higher values on the top without exception, which is line with previous studies [19, 31]. However, Kowalska et al. [36] noted the greatest microhardness values for TPF in the middle layer of the 3-mm thick 6-mm wide samples. According to this finding it is supposed that the DC simultaneously may be higher in the middle of our samples. This assumption is based on Ferracane's findings according to which an increase in hardness correlates well with increases in DC during RBC polymerization [37].

FOB composition is based on the commercial RBC from the same company (Filtek Bulk Fill Posterior Restorative, 3M ESPE, St. Paul MN, USA) with CQ/amine photoinitiator system. The organic matrix is composed of UDMA, AUDMA and DDDMA monomers, and additionally containing AFCT molecules, namely AFM. Increasing DC values corresponding to increasing radiant exposure was detected at the bottom of the groups of FOB, however, the DC value was much lower with the 3 s curing for this bulk-fill RBC compared to TPF. The high particulate filler load and the presence of Zr-silica clusters may act as obstacles in chain propagation of polymers [38]. Additionally, Feng et al. concluded that higher irradiance and shorter exposure time is intrinsically associated with a higher free radical termination rate resulting in insufficient conversion [7]. Furthermore, it was demonstrated that RBCs containing CQ/amine initiator system have lower conversion if a dual-peak LCU, like Bluephase PowerCure is used for polymerization [39]. Besides the effect of fillers and photoinitiators, the matrix content has also a great impact on the polymerization kinetics. Shah et al. found that gradual reduction in polymerization kinetics along with a steady decrease of the reaction rate by bimolecular termination is detectable by the incorporation of AFM to the resin system leading to a lower conversion [20].

Although the radiant exposure delivered by the turbo mode (5 s) was almost the same, the DCs differed significantly. In the case of FOB_10 however, the difference in DC was insufficient to reach a significant value despite the higher radiant exposure. Likewise, the DC value for FOB_20 was significantly higher compared to the group exposed to 10 s irradiation, it has failed also to reach the expected maximum value of FOB represented by the control group. Meanwhile the DC values of the top surface did not follow the above-mentioned trend at all. Surprisingly, the highest DC values were achieved at the top by the 3 s and 20 s exposure duration without a significant difference, followed by the control group, then FOB_5 and FOB_10. The top to bottom DC ratio was quite low except for the control group. These results cannot support the assumption that many RBCs receiving a high radiant exposure will follow exposure reciprocity and, consequently, have been polymerized to a high DC value [4]. Decreased DC from the surface to the bottom may be a result of the limited penetration of violet light component compared to the blue light of the polywave beam as it was mentioned above [40, 41]. Shimokawa et al. detected, that approximately 10% of the radiant power delivered to the top reached the bottom of the 4-mm RBC specimen [42]. Additionally, CQ has significantly less intense absorption compared to alternative photoinitiators [43]. On the other hand, high molecular weight monomers, such as aromatic UDMA increases the viscosity leading to decreased reactive group in the resin, which negatively influences the DC [44]. Although it was reported that CQ needs a setting time of minimum 8 s – contrary to germanium-based initiators, which set after 3-5 s exposure time – the highest DC was found at the top surface of the FOB_3 group [43]. Selig et al. found that if the initiation rate is too high due to the high irradiance, many of the free radicals that are generated are prematurely lost via bimolecular termination [45]. Probably, this is what happened at the top of the AFM-containing FOB samples.

On comparing the DC values of the two investigated RBCs, TPF was found to achieve higher DC at the bottom of the samples. This is in line with the finding of Randolph et al., who detected significantly higher final DCs in TPO-containing RBCs compared to CQ controls for irradiation times equal to or greater than 3 s [34]. Leprince et al. investigated the relation between the photoinitiator type and applicability of the exposure reciprocity law and found that TPO containing RBCs exhibited higher DC values by increasing irradiance and reducing exposure time, whilst an opposite trend was observed for CQ-based RBCs [8]. Meanwhile, irrespective of the exposure duration and irradiance, our results showed higher DC values for all FOB

groups at the top surface. It is speculated that heat conducted by the high irradiance level or high radiant exposure increased the reactivity of the AFM containing matrix system leading to an increased DC, however the more stable reactive groups or radicals of AFM are not able to efficiently propagate polymerization to the deeper layers [20].

In this study a 6-mm in diameter mold was used to represent a frequent clinical situation when the cavity orifice is smaller than the exit diameter of the light guide (10 > 9 mm for Bluephase PowerCure). Improper curing conditions, like small orifice of a conservatively prepared cavity can lead to insufficient polymerization due to limitation of light penetration [46]. The 6-mm orifice of the mold used in our study reduced the delivered radiant exposure by ~20%. In a clinical situation it must be taken into account that due to the narrow orifice of a cavity, less energy is delivered to the material to be polymerized.

The evaluation of DC was complemented by the determination of the amount of eluted monomers as it is known to correlate with the extent of polymerization [3, 47]. In vitro studies prove the cytotoxic and adverse reactions of resin monomers, which might be reduced by more complete polymerization [24, 48]. During our experiment, aromatic (BisGMA) and aliphatic (TEGDMA, UDMA, DDDMA and TCDDMA) dimethacrylate standard monomers were used to identify eluted monomers from the investigated RBCs. In addition to the monomers specified by the manufacturers, other eluted methacrylates were also detected from both TPF (TEGDMA) and FOB (BisGMA). This is consistent with the findings of other studies that the manufacturer's description or safety data sheet is incomplete with regard to the composition of the RBCs [3, 49].

According to our results, monomer elution gradually followed the increasing exposure duration with inverse proportionality, and showed statistically significant difference among the groups both for TPF and FOB. Although the radiant exposure did not differ between 3s and 5s groups, the detected monomer elution was significantly less in the latter for both RBCs. It is in line with the measured DC values at the top and bottom of TPF, however, it is valid only for the bottom DC of FOB. Kopperud et al. also demonstrated inferior curing depth and increased leaching of monomers as a result of the application of reduced polymerization time with a high intensity curing unit by testing a CQ-based and a TPO-based RBC; meanwhile, the surface properties of restorative composites were not strongly influenced by too short exposure times [49]. Controversially, Randolph et al. found increased conversion and 4 times reduced elution

from TPO-based RBC compared to CQ-based RBC with ultra-fast light curing [33]. On comparison of the investigated RBCs in our study, the total elution of monomers showed minimum 3 to 4-fold greater value in the groups of TPO-based TPF. UDMA, one of the monomers present in both materials, showed a similar degree of elution. Among the monitored monomers, BisGMA eluted at the highest level from both RBCs despite the fact that BisGMA is not included in the instructions for use and in the material safety data sheets of FOB. The strong intramolecular hydrogen bonding results in increased viscosity and decreased reactivity and mobility of BisGMA during the polymerization process. As it was demonstrated by Sideridou et Karabela the polymerization reactivity of different monomers increases in the following order: BisGMA < BisEMA < UDMA < TEGDMA [50]. This might be one of the explanations for the high elution rate of BisGMA. Even though TEGDMA is not listed as a component of TPF, it was eluted in relatively large quantities. Previous studies also detected increased amount of eluted TEGDMA caused by its low molecular weight and high mobility, resulting in a higher and faster rate of elution [23, 51].

Three-dimensional (3D) high-resolution micro-computed tomography quantitative analysis was conducted to determine the closed porosity volume in the investigated RBCs before and after polymerization. The accuracy of this method also allows for visualization of failures, such as air bubbles [52]. The measured closed porosity values were 3.5-4.5-fold lower for FOB compared to those of TPF. Submicron pores are present in the RBC as supplied from the manufacturer, while occasional larger bubbles or voids might occur during handling [53]. This is supported by our results which showed presence of pores in both RBCs before polymerization. Porosity is a parameter that affects numerous properties of filling materials. From a mechanical perspective, air incorporation represents defects in material as it is a discontinued phase of the RBC [54]. From a chemical point of view pores are lined with oxygen-inhibited layer, which is similar in composition to those of the uncured resin with consumed or reduced amounts of photoinitiator [55]. RBCs with higher pore volume may leach more unreacted monomers [56]. This is supported by our results as TPF showed higher unreacted monomer elution with higher closed porosity volume. These porosities may also contribute to an increase in water absorption capacity and consequently facilitates dissolution and hydrolysis of the constituents [57]. Porosity is not only a handling-dependent phenomenon, but is also influenced by the composition and the polymerization kinetics of the RBC. Radical

chain growth polymerization is considered to provide less controlled and heterogeneous network architecture [9, 11]. The components of the organic matrix (i.e. TEGDMA content) further influence the network heterogeneity [58]. This heterogeneity tends to increase the presence of microporosities existing between clusters of polymer chains [56]. Although, both investigated RBCs contain an AFCT molecule to rearrange network configuration providing a more homogeneous polymer architecture, our results showed an increased closed porosity after polymerization. This increase however was only significant in groups polymerized for 3 s for both RBCs. Hayashi et al. also demonstrated increased internal defect formation during polymerization, however the rapid curing setting (3 s and 3000 mW/cm^2) showed smaller defect formation compared to the conventional settings [19]. Rapid initiation induces high concentration of free radicals, which may annihilate each other resulting in reduced propagation, broad chain-length distribution, and ill-defined end-groups with increased porosity, decreased DC, and unreacted monomers trapped within the polymer network [12]. The above phenomenon was reflected by our results obtained from groups with 3 s irradiation.

Both RBCs contain AFCT molecules to reduce the stress generated by the polymerization shrinkage, although the nature of these molecules are different. The shrinkage of volumetric loss (%) in our study was determined using micro-computed tomography measurements [59]. The results showed 1.8-2.5% polymerization shrinkage values for both materials without significant difference between the groups of both RBCs despite the differences found in DC values. It is commonly reported in the literature, that monomer conversion is directly proportional to volumetric shrinkage [60], which is supported by the present results, however not in a significant manner for polymerization shrinkage. The presented shrinkage values are comparable to other findings in which other bulk-fill RBCs were tested [61]. On comparing the shrinkage between the groups of FOB and TPF, statistically a significant difference was only detected between groups irradiated for 3 s. Rapid irradiation resulted in the lowest polymerization shrinkage (1.8%) in case of TPF. This can be attributed to the lowest DC value attained for this material by using the 3-s curing. Consistent with our results, Algamaiah et al. reported, that shrinkage strain of TPF were comparable regardless of the irradiation protocol. In that study the lowest shrinkage strain arose from a 3-s protocol which may be as a consequence of incorporated β-allyl sulphone chain-transfer agent [62]. On the contrary, Par et al. reported significantly lower linear shrinkage in FOB compared to TPF, meanwhile there

was no significant difference between the shrinkage values achieved with rapid or conventional irradiation [17]. The published shrinkage values of the above study were comparable to our data [17].

5. Conclusion

Within the limitations of this *in vitro* investigation, it could be concluded that rapid 3-s polymerization resulted in reduced degree of conversion at the bottom of the AFCT modified RBCs compared to the curing protocols that provided higher radiant exitance. TPF with alternative photoinitiators achieved higher R-DC% values compared to the CQ-based FOB RBC. Monomer elution from the investigated RBCs decreased as the exposure time was reduced. Internal porosity of FOB was found to be lower compared to TPF, however significantly higher pore volume was detected after rapid polymerization. Polymerization shrinkage was comparable among groups for both RBCs with no differences across different light irradiation protocols, however, TPF showed lower shrinkage with rapid curing compared to FOB.

Acknowledgments

This work was supported by the Bolyai János Research Scholarship (BO/713/20/5); the ÚNKP-22-5 New National Excellence Program of the Ministry for Innovation and Technology from the Source of the National Research, Development and Innovation Fund (ÚNKP-22-5-PTE-1733); PTE-ÁOK-KA-2020/24 and TKP2021-EGA-17.

References

1. Rueggeberg FA, Caughman WF, Curtis Jr JW. Effect of light intensity and exposure duration on cure of resin composite. Oper Dent 1994;19:26–32.
2. Palagummi SV, Hong T, Wang Z, Moon CK, Chiang MYM. Resin viscosity determines the condition for a valid exposure reciprocity law in dental composites. Dent Mater 2020;36:310-9.
3. Lempel E, Czibulya Z, Kunsági-Máté S, Szalma J, Sümegi B, Böddi K. Quantification of conversion degree and monomer elution from dental composite using HPLC and micro-Raman spectroscopy. Chromatographia 2014;77:1137–44.
4. Feng L, Suh BI. Exposure reciprocity law in photopolymerization of multi-functional acrylates and methacrylates. Macromol Chem Phys 2007;208:295–306.

5. Rueggeberg FA. State-of-the-art: dental photocuring—a review. Dent Mater 2011;27:39–52.
6. Musanje L, Darvell BW. Polymerization of resin composite restorative materials: exposure reciprocity. Dent Mater 2003;19:531–41.
7. Feng L, Carvalho R, Suh BI. Insufficient cure under the condition of high irradiance and short irradiation time. Dent Mater 2009;25:283–9.
8. Leprince JG, Hadis M, Shortall AC, Ferracane JL, Devaux J, Leloup G, Palin WM. Photoinitiator type and applicability of exposure reciprocity law in filled and unfilled photoactive resins. Dent Mater 2011;27:157–64.
9. Hadis M, Leprince JG, Shortall AC, Devaux J, Leloup G, Palin WM. High irradiance curing and anomalies of exposure reciprocity law in resin-based materials. J Dent 2011;39:549–57.
10. Wydra JW, Cramer NB, Stansbury FW, Bowman CN. The reciprocity low concerning light dose relationships applied to BisGMA/TEGDMA photopolymers: theoretical analysis and experimental characterization. Dent Mater 2014;30:605–12.
11. da Silva EM, Poskus LT, Guimaraes JG, de Araujo Lima Barcellos A, Fellows CE. Influence of light polymerization modes on degree of conversion and crosslink density of dental composites. J Mater Sci Mater Med 2008;19:1027–32.
12. Moad CL, Moad G. Fundamentals of reversible addition–fragmentation chain transfer (RAFT). Chemistry Teacher International 2021;3:3-17.
13. Kloxin CJ, Scott TF, Bowman CN. Stress relaxation via addition-fragmentation chain transfer in a thiol-ene photopolymerization. Macromolecules 2009;42:2551-6.
14. Gorsche C, Koch T, Moszner N, Liska R. Exploring the benefits of β-allyl sulfones for more homogeneous dimethacrylate photopolymer networks. Polym Chem 2015;6:2038–47.
15. Ilie N, Watts DC. Outcomes of ultra-fast (3 s) photo-cure in a RAFT-modified resin-composite. Dent Mater 2020;36:570–9.
16. Algamaiah H, Silikas N, Watts DC. Conversion kinetics of rapid photo-polymerized resin composites. Dent Mater 2020;36:1266–1274.
17. Par M, Marovic D, Attin T, Tarle Z, Taubock TT. Effect of rapid high-intensity light-curing on polymerization shrinkage properties of conventional and bulk-fill composites. J Dent 2020;101:103448.
18. Par M, Marovic D, Attin T, Tarle Z, Taubock TT. The effect of rapid high-intensity light-curing on micromechanical properties of bulk-fill and conventional resin composites. Sci Rep 2020;10:10560.
19. Hayashi J, Tagami J, Chan D, Sadr A. New bulk-fill composite system with high irradiance light polymerization: Integrity and degree of conversion. Dent Mater 2020;36:1615–23.
20. Shah PK, Stansbury JW, Bowman CN. Application of an addition-fragmentation-chain transfer monomer in di(meth)acrylate network formation to reduce polymerization shrinkage stress. Polym Chem 2017;8:4339-51.
21. Graf N, Ilie N. Long-Term Stability of a RAFT Modified Bulk-Fill Resin-Composite under Clinically Relevant versus ISO-Curing Conditions. Materials 2020;13:5350.

22. Musanje L, Darvell BW. Curing-light attenuation in filled-resin restorative materials. Dent. Mater 2006;22:804–17.
23. Lempel E, Czibulya Zs, Kovács B, Szalma J, Tóth Á, Kunsági-Máté S, Varga Z, Böddi K. Degree of conversion and BisGMA, TEGDMA, UDMA elution from flowable bulk fill composites. Int J Mol Sci 2016;17:732.
24. Lovász BV, Lempel E, Szalma J, Sétáló Gy Jr, Vecsernyés M, Berta G. Influence of TEGDMA monomer on MMP-2, MMP-8, and MMP-9 production and collagenase activity in pulp cells. Clin Oral Investig 2021;25:2269-79.
25. Murray PE, Garcia Godoy C, Garcia Godoy F. How is the biocompatibility of dental biomaterials evaluated? Med Oral Pathol Oral Chir Buccal 2007;12:E258–E266.
26. Marovic D, Par M, Crnadak A, Sekelja A, Mandic VN, Gamulin O, Rakić M, Tarle Z. Rapid 3 s curing: What happens in deep layers of new bulk-fill composites? Materials 2021; 14:505.
27. Emami N, Söderholm KJ. How light irradiance and curing time affect monomer conversion in light-cured resin composites. Eur J Oral Sci 2003;111:536-542.
28. Peutzfeldt A, Asmussen E. Resin composite properties and energy density of light cure. J Dent Res 2005;84(7):659-662.
29. de Cássia Romano B, Soto-Montero J, Rueggeberg F, Giannini M. Effect of extended light exposure times and measurement methods on depth of cure analyses of conventional and bulk fill composites. Eur J Oral Sci 2020;128:336-44.
30. Dougherty MM, Lien W, Mansell MR, Risk DL, Savett DA, Wandewalle KS. Effect of high-intensity curing lights on the polymerization of bulk-fill composites. Dent Mater 2018;34:1531–41.
31. Lempel E, Őri Zs, Szalma J, Lovász VB, Kiss A, Tóth Á, Kunsági-Máté S. Effect of exposure time and pre-heating on the conversion degree of conventional, bulk-fill, fiber reinforced and polyacid-modified resin composites. Dent Mater 2019;35:217-28.
32. Kowalska A, Sokolowski J, Bociong K. The photoinitiators used in resin based dental composite — A review and future perspectives. Polymers 2021;13:470.
33. Randolph LD, Palin WM, Bebelman S, Devaux J, Gallez B, Leloup G, Leprince JG. Ultra-fast light-curing resin composite with increased conversion and reduced monomer elution. Dent Mater 2014;30:594–604.
34. Randolph LD, Palin WM, Watts DC, Genet M, Devaux J, Leloup G, Leprince JG. The effect of ultra-fast photopolymerisation of experimental composites on shrinkage stress, network formation and pulpal temperature rise. Dent Mater 2014;30:1280–9.
35. Par M, Repusic I, Skenderovic H, Milat O, Spajic J, Tarle Z. The effects of extended curing time and radiant energy on microhardness and temperature rise of conventional and bulk-fill resin composites. Clin Oral Investig. 2019;23:3777–788.
36. Kowalska A, Sokolowski J, Gozdek T, Krasowski M, Kopacz K, Bociong K. The influence of various photoinitiators on the properties of commercial dental composites. Polymers 2021;13:3972.
37. Ferracane JL. Correlation between hardness and degree of conversion during the setting reaction of unfilled dental restorative resins. Dent Mater 1985;1:11-4.

38. Pratap B, Gupta RK, Bhardwaj B, Nag M. Modeling based experimental investigation on polymerization shrinkage and micro-hardness of nano alumina filled resin based dental material. J Mech Behav Biomed Mater 2019;99:86-92.
39. Lucey SM, Santini A, Roebuck EM. Degree of conversion of resin-based materials cured with dual-peak orsingle-peak LED light-curing units. Int J Paediatr Dent 2015;25:93-102.
40. Sampaio CS, Atria PJ, Rueggeberg FA, Yamaguchi S, Giannini M, Coelho PG, Hirata R, Puppin-Rontani RM. Effect of blue and violet light on polymerization shrinkage vectors of a CQ/TPO-containing composite. Dent Mater 2017;33:796–804.
41. Shortall AC, Price RB, MacKenzie L, Burke FJT. Guidelines for the selection, use, and maintenance of LED light-curing units - Part 1. Br Dent J. 2016;221:453–60.
42. Shimokawa CAK, Turbino ML, Giannini M, Braga RR, Price RB. Effect of light curing units on the polymerization of bulk fill resin-based composites. Dent Mater 2018;34:1211-21.
43. Moszner N, Karl U, Ganster B, Liska R, Rheinberger V. Benzoyl germanium derivatives as novel visible light photoinitiators for dental materials. Dent Mater 2007;4:901–7.
44. Barszczewska-Rybarek. The role of molecular structure on impact resistance and bending strength of photocured urethane-dimethacrylate polymer networks. Polym Bull 2017, 74, 4023–40.
45. Selig D, Haenel T, Hausnerová B, Moeginger B, Labrie D, Sullivan B, Price RBT. Examining exposure reciprocity in a resin based composite using high irradiance levels and real-time degree of conversion values. Dent Mater 2015;31:583–93.
46. Erickson RL, Barkmeier WW. Curing characteristics of a composite. Part 2: the effect of curing configuration on depth and distribution of cure. Dent Mater 2014;30:e134–45.
47. Moldovan M, Balazsi R, Soanca A, Roman A, Sarosi C, Prodan D, Vlassa M, Cojocaru I, Saceleanu V, Cristescu I. Evaluation of the degree of conversion, residual monomers and mechanical properties of some light-cured dental resin composites. Materials 2019;12:2109
48. Goldberg M. In vitro and in vivo studies on the toxicity of dental resin components: a review. Clin Oral Investig 2008;12:1-8.
49. Kopperud HM, Johnsen GF, Lamolle S, Kleven IS, Wellendorf H, Haugen HJ. Effect of short LED lamp exposure on wear resistance, residual monomer and degree of conversion for Filtek Z250 and Tetric EvoCeram composites. Dent Mater 2013;29:824–34.
50. Sideridou ID, Karabela MM. Effect of the amount of 3-methacryloxypropyltrimethoxysilane coupling agent on physical properties of dental resin nanocomposites. Dent Mater 2009; 25:1315–24.
51. Cebe MA, Cebe F, Cengiz MF, Cetin AR, Arpag OF, Ozturk B. Elution of monomer from different bulk fill dental composite resin. Dent Mater 2015;31:141–149.
52. Sun J, Lin-Gibson S. X-ray microcomputed tomography for measuring polymerization shrinkage of polymeric dental composites. Dent Mater 2008;24:228–34.
53. Ironside JG, Makinson OF. Resin restorations: Causes of porosities. Quintessence Int 1993;24:867-73.
54. Nilsen BW, Mouhat M, Jokstad A. Quantification of porosity in composite resins delivered by injectable syringes using X-ray microtomography. Biomater Investig Dent 2020;7:86-95.

55. Gauthier MA, Stangel I, Ellis TH, Zhy XX. Oxygen inhibition in dental resins. J Dent Res 2005; 84: 725–729.
56. Balthazard R, Jager S, Dahoun A, Gerdolle D, Engels-Deutsch M, Mortie E. High-resolution tomography study of the porosity of three restorative resin composites. Clin Oral Investig 2014;18:1613-8.
57. Santerre JP, Shajii L, Leung BW. Relation of dental composite formulations to their degradation and the release of hydrolyzed polymeric-resin-derived products. Crit Rev Oral Biol Med. 2001;12:136–51.
58. Rey L, Duchet J, Galy J, Sautereau H, Vouagner D, Carrion L. Structural heterogeneities and mechanical properties of vinyl/dimethacrylate networks synthesized by thermal free radical polymerization. Polymer 2002;43:4375–84.
59. Ersen KA, Gürbüz Ö, Özcan M. Evaluation of polymerization shrinkage of bulk-fill resin composites using microcomputed tomography. Clin Oral Investig 2020;24:1687–93.
60. Kaisarly D, Gezawi ME. Polymerization shrinkage assessment of dental resin composites: A literature review. Odontology. 2016;104:257–70.
61. Shibasaki S, Takamizawa T, Nojiri K, Imai A, Tsujimoto A, Endo H, Suzuki S, Suda S, Barkmeier WW, Latta MA, Miyazaki M. Polymerization behavior and mechanical properties of high-viscosity bulk fill and low shrinkage resin composites. Oper Dent 2017;42:E177-E187.
62. Algamaiah H, Silikas N, Watts DC. Polymerization shrinkage and shrinkage stress development in ultra-rapid photo-polymerized bulk fill resin composites. Dent Mater 2021;37:559-67.

Captions

Table 1 – Materials, manufactures and compositions of bulk-fill resin composites

Table 2 – Methods of polymerization and group codes of the investigated materials

Table 3 – Differences in DC% (S.D.) of top and bottom surfaces of the investigated materials analyzed by Paired-sample t-test

Table 4 - Comparison of mean DC% on the bottom and top surfaces of Tetric PowerFill samples polymerized using different parameters of exposure. One-way analysis of variance (ANOVA) and Tukey's post hoc adjustment

Table 5 - Comparison of mean DC% on the bottom and top surfaces of Filtek One Bulk Restorative samples polymerized using different parameters of exposure. One-way analysis of variance (ANOVA) and Tukey's post hoc adjustment

Figure 1. Degree of conversion of the top and bottom surfaces of Filtek One Bulk Restorative polymerized with different exposure time and radiant exitance. Different capital letters denote statistically significant difference among groups within each material analyzed by One-way analysis of variance (ANOVA) and Tukey's post-hoc test.

Figure 2. Degree of conversion of the top and bottom surfaces of Tetric PowerFill polymerized with different exposure time and radiant exitance. Different capital letters denote statistically significant difference among groups within each material analyzed by One-way analysis of variance (ANOVA) and Tukey's post-hoc test.

Figure 3. Eluted monomers from Tetric PowerFill (A) and Filtek One Bulk Restorative (B) polymerized by different exposure time and radiant exitance. There is a significant difference between the groups denoted by different letters based on the One-Way ANOVA and Tukey's post-hoc test. Calibration curves of the standard monomers (C).

Figure 4. Polymerization shrinkage values reported as percentage. *mark indicates statistically significant difference between the materials according to the independent two tailed t-test. Among groups within the same material one-way ANOVA statistics did not show statistically significant difference.

Figure 5. Closed porosity values reported as percentage. *mark indicates statistically significant difference between the groups according to the independent two tailed t-test. Among groups within the same material one-way ANOVA statistics did not show statistically significant difference.

Figure 1

Click here to access/download;Figure;Figure 1.xlsx

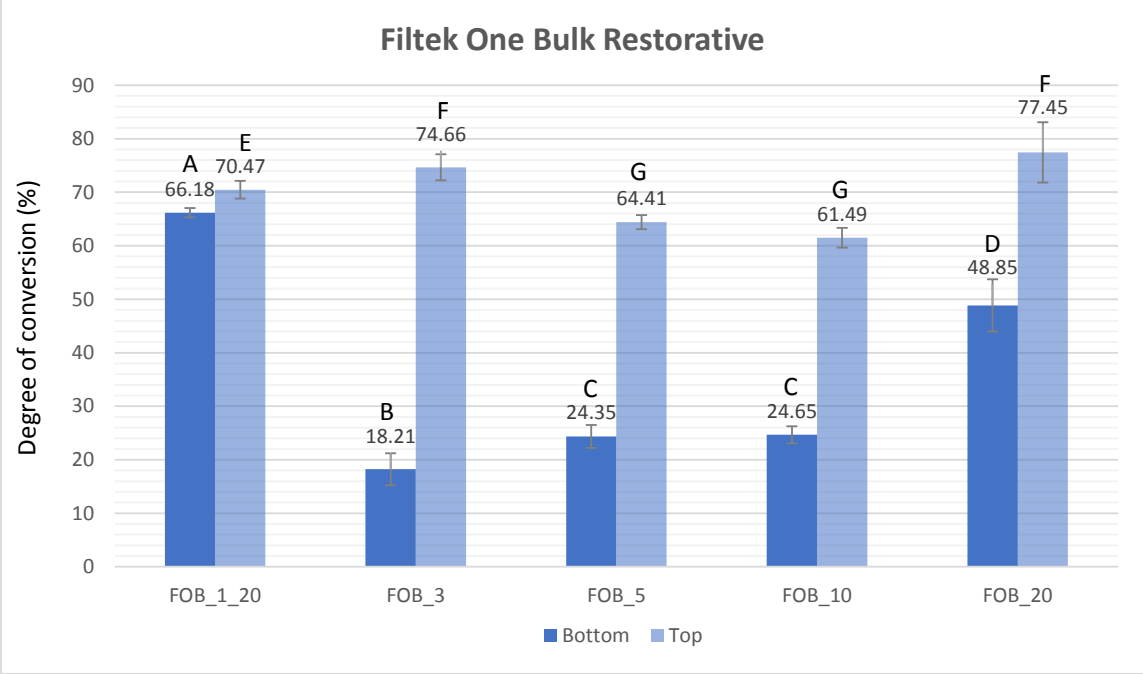

Figure 2

Click here to access/download;Figure;Figure 2.xlsx

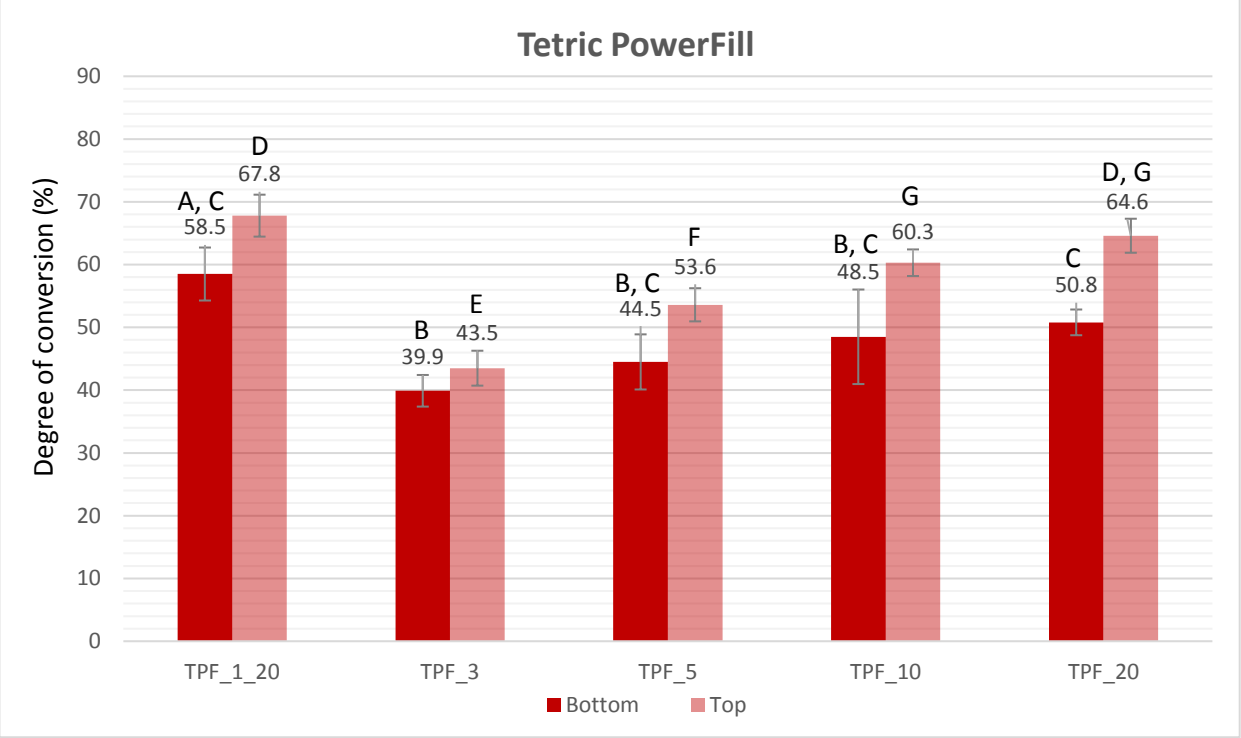

Figure 3

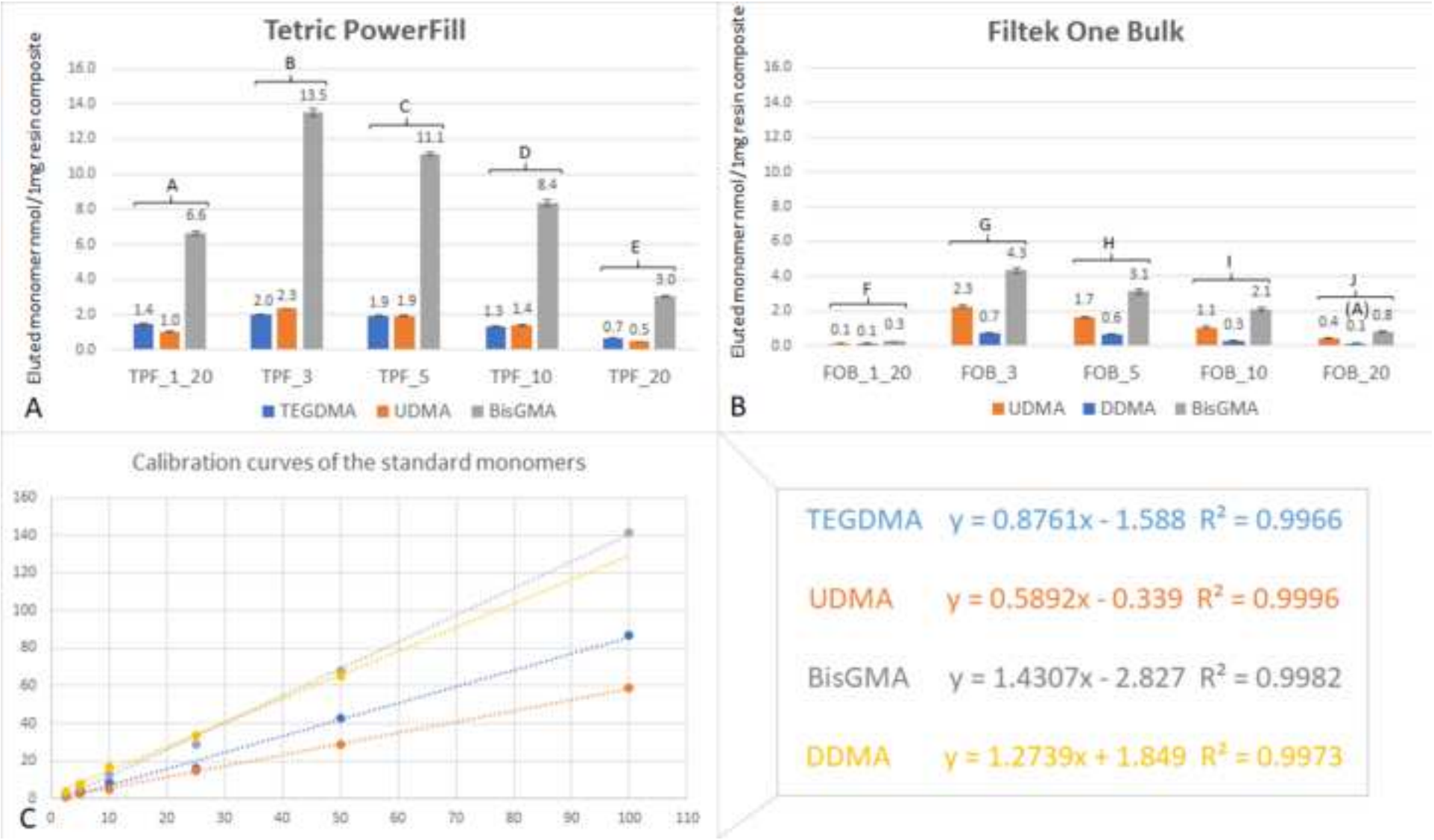

Figure 4

Click here to access/download;Figure;Figure 4.xlsx

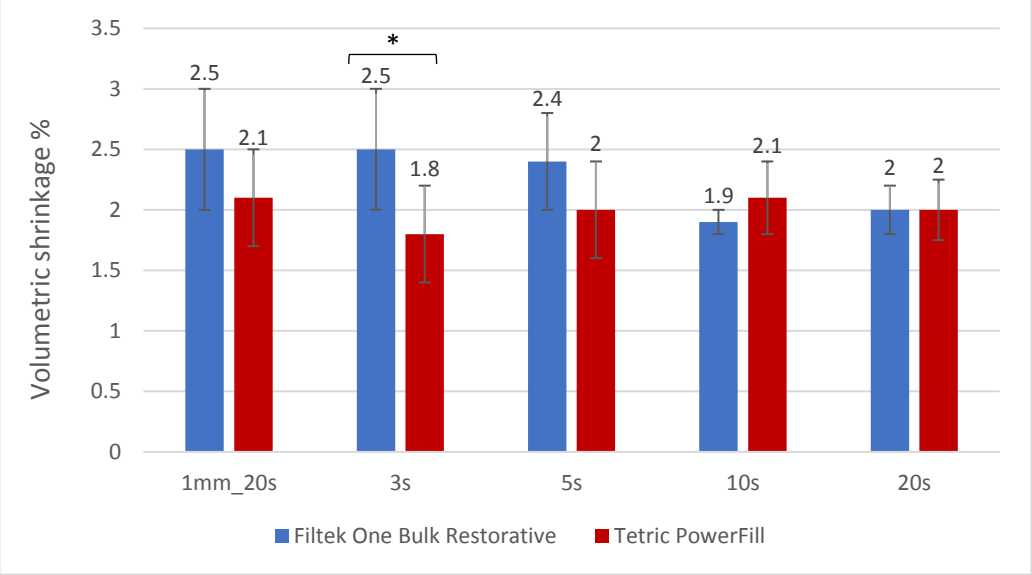

Figure 5

Click here to access/download;Figure;Figure 5.xlsx

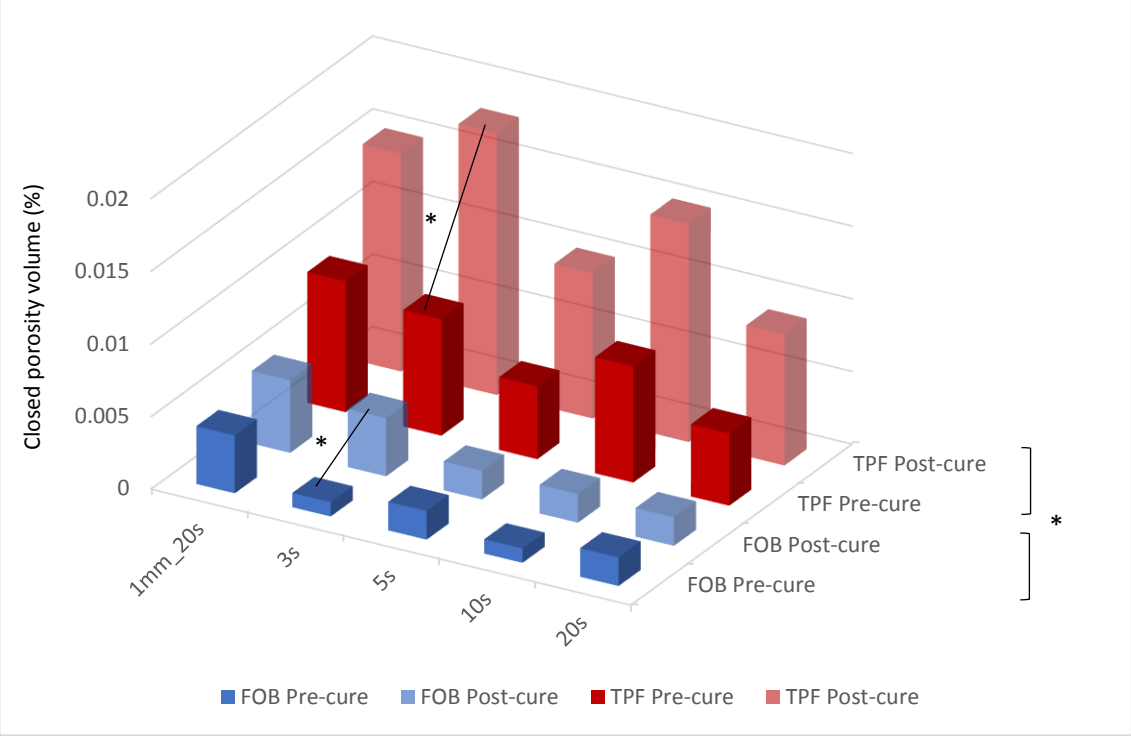

Table 1 - Materials, manufacturers and composition of bulk-fill resin-based composites

Material	Manufacturer	Resin system	Inorganic filler particles	Filler loading
Tetric PowerFill (shade: IVA)	Ivoclar Vivadent, Schaan, Liechtenstein	Bis-GMA, Bis-EMA, UDMA, TCDDMA, propoxylated bisphenol A dimethacrylate, β-allyl sulfone AFCT	barium glass, ytterbium trifluoride, mixed oxide and copolymer (40nm-3µm)	54 vol% 77 wt%
Filtek One Bulk Fill Restorative (shade: A2)	3M ESPE, St. Paul, MN, USA	AFM, UDMA, AUDMA, DDDMA	20nm silica, 4-11nm zirconia, cluster Zr-silica, 0.1µm ytterbium-trifluoride	58.5 vol% 76.5 wt%

Abbreviations: BisGMA: bisphenol-A diglycidil ether dimethacrylate; UDMA: urethane dimethacrylate; TCDDMA: tricyclodecane-dimethanol-dimethacrylate; AFCT: addition fragmentation chain transfer; AFM: addition fragmentation monomer; AUDMA: aromatic urethane dimethacrylate; DDDMA: 1,12-dodecane dimethacrylate; vol%: volume%; wt%: weight%

Table 2. Click here to access/download;Table;Table 2.xlsx

Table 2 - Parameters of polymerization and group codes of the investigated materials

Material	Layer thickness	Exposure time	Curing mode	Average irradiance (mW/cm2)	Irradiance through the 6 mm orifice of the mold (mW/cm2)	Calculated radiant exposure (J/cm^2)	Code
Tetric PowerFill (TPF)	1 mm	20 s	High	1180	938	19	TPF_1_20
	4 mm	3 s	3s	3150	2504	7.5	TPF_3
	4 mm	5 s	Turbo	1950	1550	7.8	TPF_5
	4 mm	10 s	High	1180	938	9.4	TPF_10
	4 mm	20 s	High	1180	938	19	TPF_20
Filtek One Bulk Fill Restorative (FOB)	1 mm	20 s	High	1180	938	19	FOB_1_20
	4 mm	3 s	3s	3150	2504	7.5	FOB_3
	4 mm	5 s	Turbo	1950	1550	7.8	FOB_5
	4 mm	10 s	High	1180	938	9.4	FOB_10
	4 mm	20 s	High	1180	938	19	FOB_20

Table 3. Click here to access/download;Table;Table 3.xlsx

Table 3. Differences in mean DC% (S.D.) between top and bottom surfaces of the investigated

Exposure	Tetric PowerFill						Filtek One Bulk					
	Bottom mean DC (S.D.)	Top mean DC (S.D.)	t-value (df)*	p-value*	95% CI Lower	95% CI Upper	Bottom mean DC (S.D.)	Top mean DC (S.D.)	t-value (df)*	p-value*	95% CI Lower	95% CI Upper
20 s 1 mm	58.5 (4.2)	67.8 (3.3)	3.6 (4)	0.023	2.1	16.5	66.2 (0.9)	70.5 (1.6)	4.8 (4)	0.008	1.8	6.7
	R-DC: 86.3 %						R-DC: 93.9 %					
3 s	39.9 (2.5)	43.5 (2.8)	4.5 (4)	0.011	1.3	5.8	18.2 (2.9)	74.7 (2.4)	33.1 (4)	<0.001	51.7	61.2
	R-DC: 91.7 %						R-DC: 24.4 %					
5 s	44.5 (4.4)	53.6 (2.6)	5.2 (4)	0.006	4.3	14.1	24.3 (2.1)	64.4 (1.3)	28.3 (4)	<0.001	36.1	43.9
	R-DC: 83.0 %						R-DC: 37.7 %					
10 s	48.5 (7.5)	60.3 (2.1)	4.1 (4)	0.015	3.7	19.9	24.6 (1.6)	61.5 (1.8)	99.4 (4)	<0.001	35.8	37.8
	R-DC: 80.4 %						R-DC: 40.0 %					
20 s	50.8 (2.1)	64.6 (2.7)	7.9 (4)	0.001	8.9	18.7	48.9 (4.9)	77.1 (5.6)	6.2 (4)	0.003	15.6	40.7
	R-DC: 78.6 %						R-DC: 63.5 %					

Abbreviations: DC, Degree of Conversion; S.D., Standard Deviation; R-DC, Bottom to Top DC ratio; CI, Confidence Interval

Table 4. Click here to access/download;Table;Table 4.xlsx

Table 4. Comparison of mean DC% on the bottom and top surfaces of Tetric PowerFill samples polymerized using different parameters of exposure. One-way analysis of variance (ANOVA) and Tukey's post hoc adjustment

Surface	Exposure	Mean DC (S.D.)	Comparison	Mean difference	95% CI		p-value
					Lower	Upper	
Bottom	1mm_20s	58.5 (4.2)	1mm vs. 3s	18.6	9.9	27.2	<0.001
			1mm vs. 5s	14.1	5.4	22.7	0.001
	3s	39.9 (2.5)	1mm vs. 10s	10	1.4	18.7	0.018
			1mm vs. 20s	7.7	-0.9	16.4	0.093
	5s	44.5 (4.4)	3s vs. 5s	-4.5	-13.1	4.1	0.539
			3s vs. 10s	-8.5	-17.2	0.1	0.023
	10s	48.5 (7.5)	3s vs. 20s	-10.8	-19.5	2.2	0.010
			5s vs. 10s	-4.0	-12.7	4.6	0.640
	20s	50.8 (2.1)	5s vs. 20s	-6.3	-14.9	2.3	0.224
			10s vs. 20s	-2.3	-10.9	6.3	0.929
Top	1mm_20s	67.8 (3.3)	1mm vs. 3s	24.3	19.8	29.5	<0.001
			1mm vs. 5s	14.2	8.9	19.4	<0.001
	3s	43.5 (2.9)	1mm vs. 10s	7.5	2.3	12.6	0.003
			1mm vs. 20s	3.2	-2.0	8.3	0.391
	5s	53.6 (2.6)	3s vs. 5s	-10.1	-15.3	-4.9	<0.001
			3s vs. 10s	-16.8	-22.1	-11.6	<0.001
	10s	60.3 (2.1)	3s vs. 20s	-21.1	-26.3	-15.9	<0.001
			5s vs. 10s	-6.7	-11.9	-1.5	0.008
	20s	64.6 (2.7)	5s vs. 20s	-11.0	-16.2	-5.8	<0.001
			10s vs. 20s	-4.3	-9.5	-0.9	0.137

Abbreviations: DC, Degree of Conversion; S.D., Standard Deviation; CI, Confidence Interval; vs., versus

Table 5. Click here to access/download;Table;Table 5.xlsx

Table 5. Comparison of mean DC% on the bottom and top surfaces of Filtek One Bulk Restorative samples polymerized using different parameters of exposure. One-way analysis of variance (ANOVA) and Tukey's post hoc adjustment

Surface	Exposure	Mean DC (S.D.)	Comparison	Mean difference	95% CI		p value
					Lower	Upper	
Bottom	1mm_20s	66.2 (0.9)	1mm vs. 3s	48.0	42.6	53.4	<0.001
			1mm vs. 5s	41.8	36.4	47.2	<0.001
			1mm vs. 10s	41.5	36.1	46.9	<0.001
			1mm vs. 20s	17.3	11.9	22.7	<0.001
	3s	18.2 (2.9)	3s vs. 5s	-6.1	-11.5	-0.7	0.21
			3s vs. 10s	-6.4	-11.8	-1.1	0.15
			3s vs. 20s	-30.6	-36.1	-25.2	<0.001
	5s	24.3 (2.1)	5s vs. 10s	-0.3	-5.7	5.1	1.000
			5s vs. 20s	-24.5	-29.9	-19.1	<0.001
			10s vs. 20s	-24.2	-29.6	-18.8	<0.001
	10s	24.6 (1.6)	1mm vs. 3s	-4.2	-9.9	1.5	0.224
			1mm vs. 5s	6.1	0.3	11.8	0.035
			1mm vs. 10s	9.0	3.3	14.7	0.001
			1mm vs. 20s	-6.6	-12.3	-0.9	0.020
	20s	48.9 (4.9)	3s vs. 5s	10.3	4.5	15.9	<0.001
			3s vs. 10s	13.2	7.4	18.9	<0.001
			3s vs. 20s	-2.4	-8.1	3.3	0.724
			5s vs. 10s	2.9	-2.8	8.6	0.559
			5s vs. 20s	-12.6	-18.4	6.9	<0.001
			10s vs. 20s	-15.6	-21.3	-9.8	<0.001
Top	1mm_20s	70.5 (1.6)					
	3s	74.7 (2.4)					
	5s	64.4 (1.3)					
	10s	61.5 (1.8)					
	20s	77.1 (5.6)					

Abbreviations: DC, Degree of Conversion; S.D., Standard Deviation; CI, Confidence Interval; vs., versus